Chiral crossover, deconfinement, and quarkyonic matter within a Nambu–Jona-Lasinio model with the Polyakov loop

H. Abuki,[1,2,*] R. Anglani,[1,2,+] R. Gatto,[3,‡] G. Nardulli,[1,2] and M. Ruggieri[1,2,§]

[1]*I.N.F.N., Sezione di Bari, I-70126 Bari, Italy*

[2]*Università di Bari, I-70126 Bari, Italy*

[3]*Département de Physique Théorique, Université de Genève, CH-1211 Genève 4, Switzerland*

(Received 20 May 2008; published 29 August 2008)

We study the interplay between the chiral and the deconfinement transitions, both at high temperature and high quark chemical potential, by a nonlocal Nambu–Jona-Lasinio model with the Polyakov loop in the mean field approximation and requiring neutrality of the ground state. We consider three forms of the effective potential of the Polyakov loop: two of them with a fixed deconfinement scale, cases I and II, and the third one with a μ dependent scale, case III. In cases I and II, at high chemical potential μ and low temperature T, the main contribution to the free energy is due to the $Z(3)$-neutral three-quark states, mimicking the quarkyonic phase of the large N_c phase diagram. On the other hand, in case III the quarkyonic window is shrunk to a small region. Finally we comment on the relations of these results to lattice studies and on possible common prospects. We also briefly comment on the coexistence of quarkyonic and color superconductive phases.

DOI: 10.1103/PhysRevD.78.034034 PACS numbers: 12.38.Aw, 11.10.Wx, 11.30.Rd, 12.38.Gc

I. INTRODUCTION

Color confinement and chiral symmetry breaking are some of the most intriguing topics in modern theoretical physics. Quantum chromodynamics (QCD) is believed to be the ultimate theory describing strong interactions. Nowadays it is accepted that the main ground state properties of QCD can be described in terms of nonperturbative spontaneous breaking and/or restoring of some of the global symmetries of the QCD Lagrangian.

Unfortunately, solving QCD in its nonperturbative regime is a hard task. At zero and small quark chemical potential μ lattice calculations are a good tool to derive the equation of state of QCD matter, the transition temperatures, and so on starting from the first principles; see, for example, [1–4], and references therein. Several approximation methods are available to overcome the sign problem of the fermion determinant with three colors at finite μ (see Refs. [5–7] for reviews on the sign problem): small-μ expansion [8–10], reweighting tecniques [11,12], density of the states methods [13], and analytic continuation to imaginary chemical potential [14–18].

Besides lattice calculations, effective descriptions of QCD exist. Among them Nambu–Jona-Lasinio (NJL) models [19] are very popular; see [20] for reviews. They are based on the observation that several properties of the QCD ground state are related to the spontaneous breaking of some of the global symmetries of the QCD Lagrangian. Therefore, one hopes that by a model that has the same global symmetry breaking of QCD one can capture the essential physics of QCD itself.

In recent years it has been argued that the NJL model, which does not contain gluons, can be improved by adding a nonlinear term to the Lagrangian which describes the dynamics of the traced Polyakov loop [21], and an interaction term of the Polyakov loop with the quarks. The resulting model is called the PNJL model, introduced in Refs. [22,23] and extensively studied in [24–44]. In the PNJL model one assumes that a homogeneous Euclidean temporal background gluon field couples to the quarks via the covariant derivative of QCD. This coupling gives rise to the interplay between the chiral condensate and the Polyakov loop. Even if it is very simple, the PNJL model turned out to be a powerful tool which allows one to compute several quantities that can be computed on the lattice as well. The agreement with existing lattice data is satisfactory [24].

One of the exciting characteristics of the PNJL model is the *statistical confinement* of quarks at low temperature.[1] In a few words this means that at small temperature and small chemical potential, the contributions to the free energy, Ω, of the states with one and two quarks are suppressed, and the leading contribution to Ω arises from the thermal excitations of colorless three-quark states. This property is related to the small value of the expectation value of the Polyakov loop which is found in the self-consistent calculations within the PNJL model in the aforementioned conditions of temperature and chemical potential.

*hiroaki.abuki@ba.infn.it
+roberto.anglani@ba.infn.it
‡raoul.gatto@physics.unige.ch
§marco.ruggieri@ba.infn.it

[1]The term statistical confinement was introduced by K. Redlich during the Workshop "New Frontiers in QCD08."

It has been shown, first by Sasaki, Friman, and Redlich in Ref. [30] and shortly after by Fukushima [33] that the statistical confinement property of the PNJL model persists even at high chemical potential [33]. This result is in agreement with the phase diagram of QCD obtained in the large number of colors N_c approximation [45,46]; see also Refs. [47,48] for recent related studies. Inspired by Ref. [45] Fukushima has suggested to interpret the statistical confined phase of the PNJL model at high quark chemical potential as the quarkyonic state found in [45].

In this work we investigate the ground state of the electrically neutral two flavor PNJL model, focusing on its possible quarkyonic structure at high μ and low T. We use a nonlocal four fermion interaction instead of the local one [19]. The local NJL model is usually regularized by means of an ultraviolet sharp cutoff, which amounts to artificially cutoff the quark momenta that are larger than the cutoff itself. Thus the extensions of the model to temperatures and/or chemical potentials of the order of the cutoff are quite dubious. However, if one introduces a nonlocal interaction, which corresponds to the multiplication of the NJL coupling by a momentum dependent form factor $f(p)$, and requires that the form factor satisfies the asymptotic freedom property of QCD $f(p \to \infty) = 0$, then all of the momentum integrals are convergent and the model is consistent at any value of temperature and chemical potential. In this paper we use one specific form of the form factor. Although the choice of a different functional form for $f(p)$ can lead to different quantitative results (mainly the shift of the critical points) we believe that our picture should not be modified qualitatively. We consider the logarithmic form of the Polyakov loop effective potential $\mathcal{U}$ suggested by Roessner, Ratti, and Weise in Ref. [25]. Moreover, we investigate the effects of a dependence of $\mathcal{U}$ on the quark chemical potential as well as on the number of flavors as suggested in Ref. [28]. We compare the phase diagrams obtained in the cases in which we do not consider (cases I and II) and do consider (case III) the μ dependence of $\mathcal{U}$. Cases I and II differ for the value of the deconfinement scale in the Polyakov loop effective potential.

We find that the phase diagrams in the two cases (I and II on one side, III on the other side) differ even qualitatively. In particular, on one hand, in cases I and II we confirm the results of Fukushima [33] and strengthen his interpretation of the high chemical potential/small temperature state of the PNJL model as the quarkyonic matter of the large N_c phase diagram. On the other hand, in case III we find that the quarkyoniclike window found in cases I and II is shrunk and becomes a small region in the $\mu - T$ plane in case III, opening a wide room for the deconfined quark matter of the pure NJL model.

The plan of the paper is as follows. In Sec. II we sketch the formalism. In Sec. III we discuss our results. Finally in Sec. IV we draw our conclusions.

II. THERMODYNAMIC POTENTIAL WITH A NONLOCAL FOUR FERMION INTERACTION

The Lagrangian density of the two flavor PNJL model is given by [23,41]

$$\mathcal{L}' = \bar{e}(i\gamma_\mu \partial^\mu)e + \bar{\psi}(i\gamma_\mu D^\mu + \mu\gamma_0 - m)\psi + \mathcal{L}_4 - \mathcal{U}[\Phi, \bar{\Phi}, T]. \tag{1}$$

In the above equation e denotes the electron field; ψ is the quark spinor with Dirac, color, and flavor indices (implicitly summed). m corresponds to the bare quark mass matrix; we assume from the very beginning $m_u = m_d$. The covariant derivative is defined as usual as $D_\mu = \partial_\mu - iA_\mu$. The gluon background field $A_\mu = \delta_{0\mu}A_0$ is supposed to be homogeneous and static, with $A_0 = gA_0^a T_a$ and T_a, $a = 1, \ldots, 8$ being the $SU(3)$ color generators with the normalization condition $\mathrm{Tr}[T_a, T_b] = \delta_{ab}$. Finally μ is the chemical mean quark chemical potential, related to the conserved baryon number.

In Eq. (1) Φ, $\bar{\Phi}$ correspond to the normalized traced Polyakov loop L and its Hermitian conjugate, respectively, $\Phi = \mathrm{Tr}W/N_c$, $\bar{\Phi} = \mathrm{Tr}W^\dagger/N_c$, with

$$W = \mathcal{P}\exp\left(i\int_0^\beta A_4 d\tau\right) = \exp(i\beta A_4), \qquad A_4 = iA_0, \tag{2}$$

and $\beta = 1/T$. Φ is a color singlet but it has a $Z(3)$ charge [21], where $Z(3)$ is the center of the color group $SU(3)$; thus if $\Phi \neq 0$ in the ground state then the $Z(3)$ symmetry is spontaneously broken. The term $\mathcal{U}[\Phi, \bar{\Phi}, T]$ is the effective potential for the traced Polyakov loop; in the absence of dynamical quarks it is built in order to reproduce the pure glue lattice data of QCD, namely, thermodynamical quantities (pressure, entropy, and energy density) and the deconfinement temperature of heavy (nondynamical) quarks, $T = 270$ MeV. Several forms of this potential have been suggested in the literature; see, for example, [23–26,33]. In this paper we adopt the following logarithmic form [25]:

$$\mathcal{U}[\Phi, \bar{\Phi}, T] = T^4\left[-\frac{b_2(T)}{2}\bar{\Phi}\Phi + b(T)\log[1 - 6\bar{\Phi}\Phi + 4(\bar{\Phi}^3 + \Phi^3) - 3(\bar{\Phi}\Phi)^2]\right], \tag{3}$$

with

$$b_2(T) = a_0 + a_1\left(\frac{\bar{T}_0}{T}\right) + a_2\left(\frac{\bar{T}_0}{T}\right)^2, \qquad b(T) = b_3\left(\frac{\bar{T}_0}{T}\right)^3. \tag{4}$$

Numerical values of the coefficients are as follows [25]:

$$a_0 = 3.51, \qquad a_1 = -2.47, \qquad a_2 = 15.2, \qquad b_3 = -1.75. \tag{5}$$

If dynamical quarks were not present then one should chose $\bar{T}_0 = 270$ MeV in order to reproduce the deconfinement transition at $T = 270$ of the pure gauge theory [23,24,29]. In the presence of quarks $\bar{T}_0$ might get a dependence on the number of active flavors as well as on the quark chemical potential [24,28]. Inspired by Refs. [23,24,28] in this paper we consider three cases:

$$\bar{T}_0 = 208 \text{ MeV}, \qquad \text{case I}, \tag{6}$$

$$\bar{T}_0 = 270 \text{ MeV}, \qquad \text{case II}, \tag{7}$$

$$\bar{T}_0(\mu) = T_\tau e^{-1/\alpha_0 c(\mu)}, \qquad \text{case III}. \tag{8}$$

Case II corresponds to the deconfinement temperature in the pure glue theory; the parameters in cases I and III have been evaluated in Ref. [28] on the basis of hard dense and hard thermal loop approximations to QCD. In the equation corresponding to case III we have set

$$\alpha_0 = 0.304, \qquad T_\tau = 1770 \text{ MeV}, \tag{9}$$

and

$$c(\mu) = \frac{11N_c - 2N_f}{6\pi} - \frac{16N_f}{\pi}\frac{\mu^2}{T_\tau^2}, \tag{10}$$

with $N_f = 2$ and $N_c = 3$. At $\mu = 0$ we have $\bar{T}_0(\mu = 0) = 208$ MeV as case I; for comparison, at $\mu = 500$ MeV the deconfinement scale is given by $\bar{T}_0(\mu = 500) = 19$ MeV.

In Eq. (1) $\mathcal{L}_4$ represents the Lagrangian density for the four fermion interaction. If we define $S_4 = \int d^4x \mathcal{L}_4$ as the interaction action, then in the local version of the NJL model one has

$$S_4 = G\int d^4x[(\bar{\psi}\psi)^2 + (\bar{\psi}i\gamma_5\boldsymbol{\tau}\psi)^2]. \tag{11}$$

In the nonlocal version of the NJL model the contact term Eq. (11) is replaced by [30,49–54]

$$S_4 = G\int d^4x[(\bar{q}(x)q(x))^2 + (\bar{q}(x)i\gamma_5\boldsymbol{\tau}q(x))^2], \tag{12}$$

where the dressed quark field is defined as

$$q(x) = \int d^4y F(x-y)\psi(y), \tag{13}$$

and $F(r)$ is a form factor whose Fourier transform $f(p)$ satisfies the constraint $f(p) \to 0$ for $p \to \infty$, with p being the 3-momentum. In this paper we follow Ref. [30] and use the Lorentzian form factor,

$$f(p) = \frac{1}{\sqrt{1 + (p/\Lambda)^{2\alpha}}}. \tag{14}$$

In the above equation $\Lambda = 684.2$ MeV and $\alpha = 10$. Moreover we use $m = 4.46$ MeV and $G = 2.33/\Lambda^2$ [30]. By these numerical values we reproduce the pion decay constant $f_\pi = 92.3$ MeV and the pion mass $m_\pi = 135$ MeV, as well as the chiral condensate $\langle\bar{u}u\rangle = -(256.2 \text{ MeV})^3$. Although the choice of a different form factor will lead to different critical temperatures and/or chemical potentials, it is quite reasonable that the qualitative picture that we draw in this work is insensitive to the specific form of $f(p)$.

As explained in the Introduction we are interested in the ground state of the model specified by the Lagrangian in Eq. (1), at each value of the temperature T and the chemical potential μ, corresponding to a vanishing total electric charge. In order to build the neutral ground state we use the standard grand canonical ensemble formalism, adding to Eq. (1) the term $\mu_Q N_Q$, μ_Q being the chemical potential (i.e., Lagrange multiplier) for the total charge N_Q, and requiring stationarity of the thermodynamic potential with respect to variations of μ_Q, which is equivalent to the requirement $\langle N_Q\rangle = 0$ in the ground state. This amounts to write the Lagrangian $\mathcal{L}$ in the grand canonical ensemble $\mathcal{L} = \mathcal{L}' + \mu_Q N_Q$ as [41]

$$\mathcal{L} = \bar{e}(i\gamma_\mu\partial^\mu + \mu_e\gamma_0)e + \bar{\psi}(i\gamma_\mu D^\mu + \hat{\mu}\gamma_0 - m)\psi + G[(\bar{\psi}\psi)^2 + (\bar{\psi}i\gamma_5\vec{\tau}\psi)^2] - \mathcal{U}[\Phi, \bar{\Phi}, T], \tag{15}$$

where $\mu_e = -\mu_Q$ and the quark chemical potential matrix $\hat{\mu}$ is defined in flavor-color space as

$$\hat{\mu} = \begin{pmatrix} \mu - \frac{2}{3}\mu_e & 0 \\ 0 & \mu + \frac{1}{3}\mu_e \end{pmatrix} \otimes \mathbf{1}_c, \tag{16}$$

where $\mathbf{1}_c$ denotes the identity matrix in color space. At $\mu_e \neq 0$ a difference of the chemical potential between up and down quarks, $\delta\mu = \mu_2/2$, arises.

In this paper we work in the mean field approximation. Because of $\delta\mu \neq 0$, a pion condensation might occur in the ground state [55]. In order to study simultaneously chiral symmetry breaking and pion condensation we assume that in the ground state the expectation values, real and independent on x, for the following operators may develop [32,41,55–58]:

$$\sigma = G\langle\bar{q}(x)q(x)\rangle, \qquad \pi = G\langle\bar{q}(x)i\gamma_5\tau_1 q(x)\rangle. \tag{17}$$

In the above equation a summation over flavor and color is understood. We have assumed that the pion condensate aligns along the τ_1 direction in flavor space. This choice is not restrictive. As a matter of fact we should allow for independent condensation both in π^+ and in π^- channels [32]:

$$\pi^\pm \equiv G\langle\bar{\psi}i\gamma_5\tau_\pm\psi\rangle = \frac{\pi}{\sqrt{2}}e^{\pm i\theta}, \tag{18}$$

with $\tau_\pm = (\tau_1 \pm \tau_2)/\sqrt{2}$, but the thermodynamical potential is not dependent on the phase θ. Therefore, we can assume $\theta = 0$ which leaves us with $\pi^+ = \pi^- = \pi/\sqrt{2}$ and introduce only one condensate, specified in Eq. (17).

In what follows we consider the system at finite temperature T in the volume V. This implies that the space-

time integral is $\int d^4x = \int_0^\beta d\tau \int d^3\boldsymbol{x}$ with $\beta = 1/T$. In the mean field approximation the PNJL action reads

$$S = \int d^4x[\bar{e}(i\gamma_\mu\partial^\mu + \mu_e\gamma_0)e + \bar{\psi}(i\gamma_\mu D^\mu + \hat{\mu}\gamma_0)\psi] + 2\sigma\int d^4x\bar{q}(x)q(x) + 2\pi\int d^4x\bar{q}(x)i\gamma_5\tau_1 q(x) - \beta V\frac{\sigma^2+\pi^2}{G} - \beta V\mathcal{U}[\Phi,\bar{\Phi},T], \tag{19}$$

where V is the quantization volume and $\beta = 1/T$. In momentum space one has

$$S = \int \frac{d^4p}{(2\pi)^4}[\bar{e}(\gamma_\mu p^\mu + \mu_e\gamma_0)e + \bar{\psi}(\gamma_\mu p^\mu - \gamma_\mu A^\mu - \hat{\mu}\gamma_0)\psi] + \int \frac{d^4p}{(2\pi)^4}f(p)^2[2\sigma\bar{\psi}(p)\psi(p) + 2\pi\bar{\psi}(p)i\gamma_5\tau_1\psi(p)] - \beta V\frac{\sigma^2+\pi^2}{G} - \beta V\mathcal{U}[\Phi,\bar{\Phi},T], \tag{20}$$

with $A_\mu = gA^a_\mu T_a$. We introduce the mean field momentum dependent constituent quark mass $M(p)$ and renormalized pion condensate $N(p)$:

$$M(p) \equiv m - 2\sigma f^2(p), \qquad N \equiv -2\pi f^2(p). \tag{21}$$

The thermodynamical potential Ω per unit volume in the mean field approximation can be obtained by integration over the fermion fields in the partition function of the model, see, for example, Ref. [56],

$$\Omega = -\left(\frac{\mu_e^4}{12\pi^2} + \frac{\mu_e^2T^2}{6} + \frac{7\pi^2T^4}{180}\right) + \mathcal{U}[\Phi,\bar{\Phi},T] + \frac{\sigma^2+\pi^2}{G} - T\sum_n\int\frac{d^3\boldsymbol{p}}{(2\pi)^3}\,\mathrm{Tr}\log\frac{S^{-1}(i\omega_n,\boldsymbol{p})}{T}, \tag{22}$$

where the sum is over fermion Matsubara frequencies $\omega_n = \pi T(2n+1)$, and the trace is over Dirac, flavor, and color indices. The inverse quark propagator is defined as

$$S^{-1}(i\omega_n,\boldsymbol{p}) = \begin{pmatrix} (i\omega_n + \mu - \frac{2}{3}\mu_e + iA_4)\gamma_0 - \boldsymbol{\gamma}\cdot\boldsymbol{p} - M(p) & -i\gamma_5 N(p) \\ -i\gamma_5 N(p) & (i\omega_n + \mu + \frac{1}{3}\mu_e + iA_4)\gamma_0 - \boldsymbol{\gamma}\cdot\boldsymbol{p} - M(p)\end{pmatrix}\otimes\mathbf{1}_c. \tag{23}$$

Performing the trace and the sum over Matsubara frequencies we have the effective potential for Φ, σ, and π, namely,

$$\begin{aligned}\Omega = &-\left(\frac{\mu_e^4}{12\pi^2} + \frac{\mu_e^2T^2}{6} + \frac{7\pi^2T^4}{180}\right) + \mathcal{U}[\Phi,\bar{\Phi},T] + \frac{\sigma^2+\pi^2}{G} - 2N_c\int\frac{d^3\boldsymbol{p}}{(2\pi)^3}[E_+ + E_- - 2p] \\ &- 2T\int\frac{d^3\boldsymbol{p}}{(2\pi)^3}\log[1 + 3\Phi e^{-\beta(E_+-\mu)} + 3\bar{\Phi}e^{-2\beta(E_+-\mu)} + e^{-3\beta(E_+-\mu)}] \\ &- 2T\int\frac{d^3\boldsymbol{p}}{(2\pi)^3}\log[1 + 3\Phi e^{-\beta(E_--\mu)} + 3\bar{\Phi}e^{-2\beta(E_--\mu)} + e^{-3\beta(E_--\mu)}] \\ &- 2T\int\frac{d^3\boldsymbol{p}}{(2\pi)^3}\log[1 + 3\bar{\Phi}e^{-\beta(E_++\mu)} + 3\Phi e^{-2\beta(E_++\mu)} + e^{-3\beta(E_++\mu)}] \\ &- 2T\int\frac{d^3\boldsymbol{p}}{(2\pi)^3}\log[1 + 3\bar{\Phi}e^{-\beta(E_-+\mu)} + 3\Phi e^{-2\beta(E_-+\mu)} + e^{-3\beta(E_-+\mu)}],\end{aligned} \tag{24}$$

where

$$E_\pm = \sqrt{(E_p \mp \mu_e/2)^2 + N^2}, \tag{25}$$

and $E_p = \sqrt{p^2 + M^2(p)}$. In Eq. (24) the integral of $2p$ is an irrelevant constant that we subtract in order to make the thermodynamical potential finite at each value of temperature and chemical potential. The ground state of the model is defined by the values of σ, π, Φ, and $\bar{\Phi}$ that minimize Ω and that have a vanishing total charge; the latter condition is equivalent to the requirement

$$\frac{\partial\Omega}{\partial\mu_e} = 0. \tag{26}$$

In this paper we use the convenient Polyakov gauge,

$$\Phi = \tfrac{1}{3}\mathrm{Tr}[e^{i\beta(\lambda_3\phi_3 + i\lambda_8\phi_8)}], \tag{27}$$

with ϕ_3, ϕ_8 being the real parameters. It has been widely discussed in Ref. [25] that in the mean field approximation and with the choice of the effective potential $\mathcal{U}$ given by Eq. (3) one has $\langle\Phi\rangle = \langle\bar{\Phi}\rangle$ for any value of T and μ, and the solution $\langle\Phi\rangle \neq \langle\bar{\Phi}\rangle$ at finite μ is due to quantum fluctuations. Since in this paper we consider only the mean field approximation we chose $\Phi = \bar{\Phi}$ in the calculations. This choice implies $\phi_8 = 0$, and thus we are left with only one parameter $\phi_3 \equiv \phi$.

Before closing this section we write the dispersion laws of the quasiparticles in the Polyakov gauge, defined as the poles of the quark propagator given by Eq. (23):

$$E_{ur} = \mp\mu \pm i\phi + E_+, \qquad E_{dr} = \mp\mu \pm i\phi + E_-, \tag{28}$$

$$E_{ug} = \mp\mu \mp i\phi + E_+, \qquad E_{dg} = \mp\mu \mp i\phi + E_-, \tag{29}$$

$$E_{ub} = \mp\mu + E_+, \qquad E_{db} = \mp\mu + E_-. \tag{30}$$

In the previous equations u, d correspond to up and down quarks, and r, g, and b to the colors red, green, and blue; the upper (lower) sign multiplying μ and ϕ corresponds to quarks (antiquarks).

III. SUSCEPTIBILITIES IN THE PNJL MODEL

In order to study the landscape of the phases of the PNJL model we introduce the susceptibility matrix. Susceptibilities are useful to identify phase transitions since they are proportional to the fluctuations of the order parameters around their mean field values, which usually are enhanced near a phase transition. We follow closely Ref. [30] for the formalism settings. The first step is the definition of the dimensionless curvature matrix of the free energy around its global minima C [23,30],

$$C \equiv \begin{pmatrix} C_{MM} & C_{M\Phi} & C_{M\bar{\Phi}} \\ C_{M\Phi} & C_{\Phi\Phi} & C_{\Phi\bar{\Phi}} \\ C_{M\bar{\Phi}} & C_{\Phi\bar{\Phi}} & C_{\bar{\Phi}\bar{\Phi}} \end{pmatrix}. \tag{31}$$

In the above equation the diagonal entries are defined as

$$C_{MM} = \frac{\beta}{\Lambda}\frac{\partial^2\Omega}{\partial M^2}, \tag{32}$$

$$C_{\Phi\Phi} = \frac{\beta}{\Lambda^3}\frac{\partial^2\Omega}{\partial\Phi^2}, \qquad C_{\bar{\Phi}\bar{\Phi}} = \frac{\beta}{\Lambda^3}\frac{\partial^2\Omega}{\partial\bar{\Phi}^2}; \tag{33}$$

with $\beta = 1/Tf$, and Λ is the mass scale defining the form factor Eq. (14). Ω is defined in Eq. (24). In what follows we denote by M the constituent quark mass computed at $p = 0$, which is a function of μ and T. The off-diagonal entries are given by

$$C_{M\Phi} = \frac{\beta}{\Lambda^2}\frac{\partial^2\Omega}{\partial\Phi\partial M}, \qquad C_{M\bar{\Phi}} = \frac{\beta}{\Lambda^2}\frac{\partial^2\Omega}{\partial\bar{\Phi}\partial M}, \tag{34}$$

$$C_{\Phi\bar{\Phi}} = \frac{\beta}{\Lambda^3}\frac{\partial^2\Omega}{\partial\Phi\partial\bar{\Phi}}; \tag{35}$$

the derivatives are computed at the global minimum of Ω. Notice that the proper definition of the curvature matrix requires that we put $\Phi = \bar{\Phi}$, namely, the mean field solution, only after differentiation.

The susceptibility matrix $\hat{\chi}$ is computed as the inverse of the curvature matrix C. We have

$$\hat{\chi} = \begin{pmatrix} \chi_{MM} & \chi_{M\Phi} & \chi_{M\bar{\Phi}} \\ \chi_{M\Phi} & \chi_{\Phi\Phi} & \chi_{\Phi\bar{\Phi}} \\ \chi_{M\bar{\Phi}} & \chi_{\Phi\bar{\Phi}} & \chi_{\bar{\Phi}\bar{\Phi}} \end{pmatrix}. \tag{36}$$

Here χ_{MM}, $\chi_{\Phi\Phi}$, and $\chi_{\bar{\Phi}\bar{\Phi}}$ denote, respectively, the dimensionless susceptibilities of the constituent quark mass, of the Polyakov loop and of its complex conjugate. We also introduce the average susceptibility

$$\bar{\chi} = \tfrac{1}{4}(\chi_{\Phi\Phi} + \chi_{\bar{\Phi}\bar{\Phi}} + 2\chi_{\Phi\bar{\Phi}}). \tag{37}$$

IV. RESULTS AND DISCUSSION

In this section we sketch our results. First we discuss the set of parameters corresponding to case I which corresponds to $\bar{T}_0 = 208$ MeV. Case II is qualitatively similar to case I; therefore, after the discussion of the results obtained in the latter case we briefly show the results corresponding to the former case. Finally we compare both qualitatively and quantitatively cases I and III. We find that the phase structures of the models corresponding to cases I and III are quite different.

A. Case I: Masses, Polyakov loop, and quarkyonic matter

In the upper panel of Fig. 1 we plot the constituent quark mass at $p = 0$, the expectation value of the traced Polyakov and the electron chemical potential as a function of the temperature, computed at $\mu = 0$ (left panel) and $\mu = 300$ MeV (right panel). M_0 denotes the constituent quark mass at $p = 0$, $\mu = 0$, $\mu_e = 0$ and $T = 0$, $M_0 = 335$ MeV. The pion condensate N is not shown since we find $N = 0$ once electrical neutrality has been imposed. The latter result is in agreement with what we have found in our previous work, see Ref. [41], where we have considered the local version of the neutral two flavor PNJL model. Even if we have shown results only for two values of the quark chemical potential, we have explicitly verified that N vanishes in the whole range of chemical potentials and temperatures considered in this work, namely, $0 \leq \mu \leq 500$ MeV and $0 \leq T \leq 250$ MeV.

The expectation value of the Polyakov loop at $\mu = 0$ is consistent with zero up to temperatures of the order of 100 MeV.[2] It rises as the temperature is increased becoming of the order of 1 for temperatures close to 250 MeV. This behavior signals a crossover from a low temperature phase with an unbroken $Z(3)$ symmetry, to a high temperature phase with $Z(3)$ symmetry spontaneously broken. The behavior of Φ as a function of the temperature is observed even at higher values of μ, see, for example, the upper right panel of Fig. 1. We call such a crossover the $Z(3)$ crossover throughout this paper.

[2] Φ cannot be exactly zero because dynamical quarks break the $Z(3)$ symmetry explicitly; nevertheless Φ turns out to be very small, signaling that the center symmetry is broken only softly.

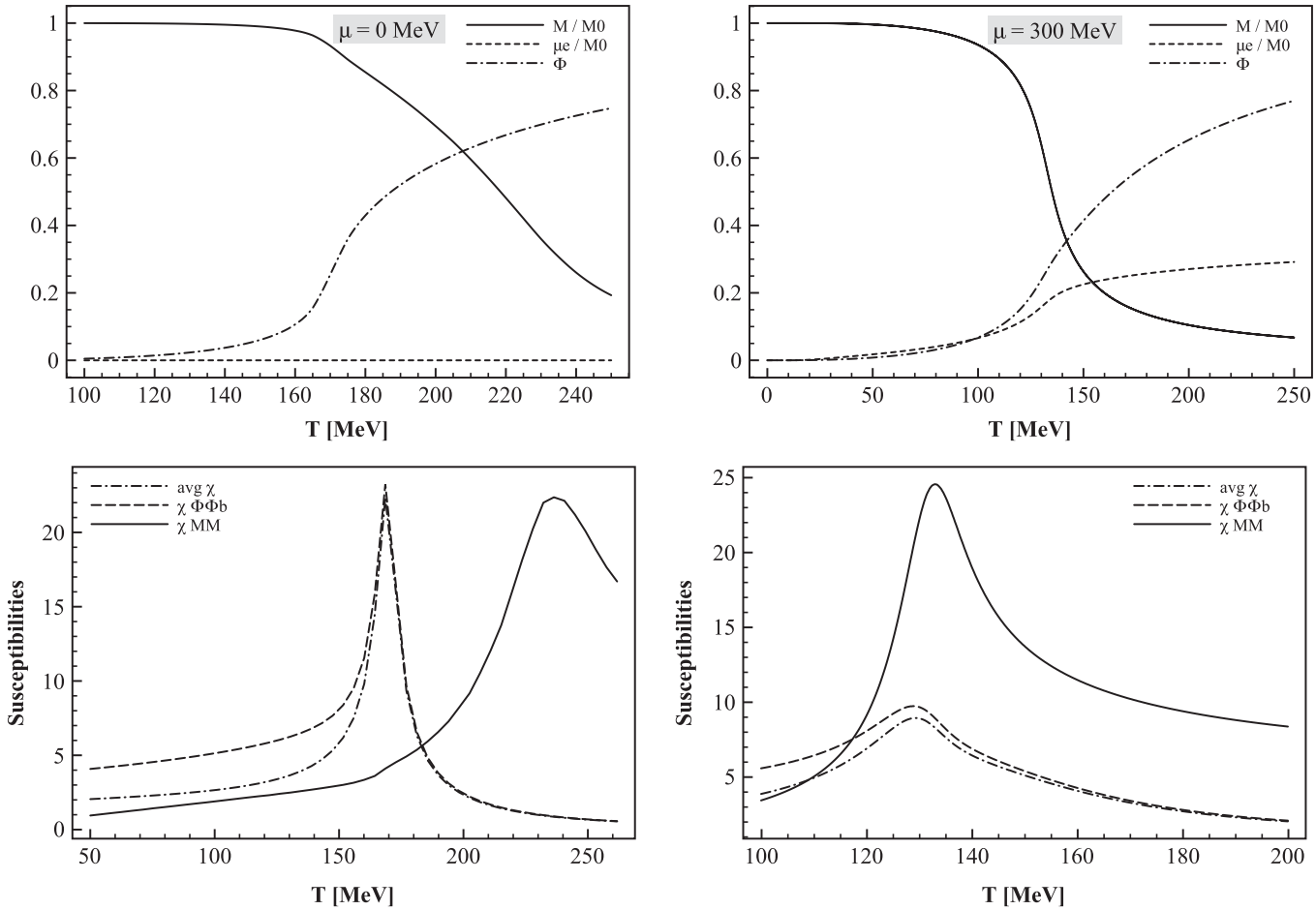

FIG. 1. Upper panel: constituent quark mass at $p = 0$, pion condensate at $p = 0$, and a Polyakov loop as a function of temperature, computed at $\mu = 0$ (left panel) and $\mu = 353.5$ MeV (right panel). M_0 denotes the constituent quark mass at $p = 0$, $\mu = 0$, $\mu_e = 0$ and $T = 0$, $M_0 = 335$ MeV. Lower left panel: susceptibilities at $\mu = 0$ as a function of temperature. Lower right panel: susceptibilities at $\mu = 300$ MeV as a function of temperature. Solid line: χ_{MM}. Dashed line: $\chi_{\Phi\bar{\Phi}}$. Dot-dashed line: $\bar{\chi}$.

In the lower panel of Fig. 1 we plot three of the susceptibilities defined in the previous section, namely, χ_{MM} (solid line), $\chi_{\Phi\bar{\Phi}}$ (dashed line), and $\bar{\chi}$ (dot-dashed line), as a function of temperature at $\mu = 0$ (left panel) and $\mu = 300$ MeV (right panel). In this work we identify the chiral crossover temperature with the temperature where χ_{MM} is maximum. In the same way and following Ref. [30] we define the $Z(3)$ crossover temperature as the one corresponding to the maximum of $\bar{\chi}$.

We wish to investigate the spontaneous breaking of the $Z(3)$ symmetry in the neutral PNJL model as the quark chemical potential is increased at a fixed low temperature. To this end we plot in Fig. 2 the constituent quark mass at $p = 0$, the expectation value of the traced Polyakov and the electron chemical potential as a function of the quark chemical potential μ, computed at $T = 20$ MeV (left panel). M_0 denotes the constituent quark mass at $p = 0$, $\mu = 0$ and $T = 0$, $M_0 = 335$ MeV. Again we do not show the pion condensate since it turns out to vanish in the neutral phase. At low temperatures we find a first order chiral transition at $\mu \approx 353$ MeV, in agreement with our previous analysis [41]. In correspondence with the chiral restoration the expectation value of the Polyakov loop has a sudden jump. Nevertheless its value remains much smaller than 1 even if μ is increased to 500 MeV, where $\Phi \approx 0.04$. For comparison we show the same quantities at $T = 130$ MeV in the right panel.

We now focus on the low temperature regime; therefore we refer to the left panel of Fig. 2. In this case we cannot identify the jump of Φ as the $Z(3)$ crossover. Instead the discontinuity of Φ is simply due to the coupling of the Polyakov loop with the chiral condensate. This is confirmed by the calculation of the Polyakov loop susceptibilities; see the lower panel of Fig. 2. At $T = 20$ MeV, in correspondence with the jump of the constituent quark mass, the chiral susceptibility has a pronounced peak. On the other hand, the Polyakov loop susceptibilities are very smooth functions of μ with a small cusp in correspondence with the chiral transition, signaling the absence of a phase transition (as well as of a crossover). For comparison we

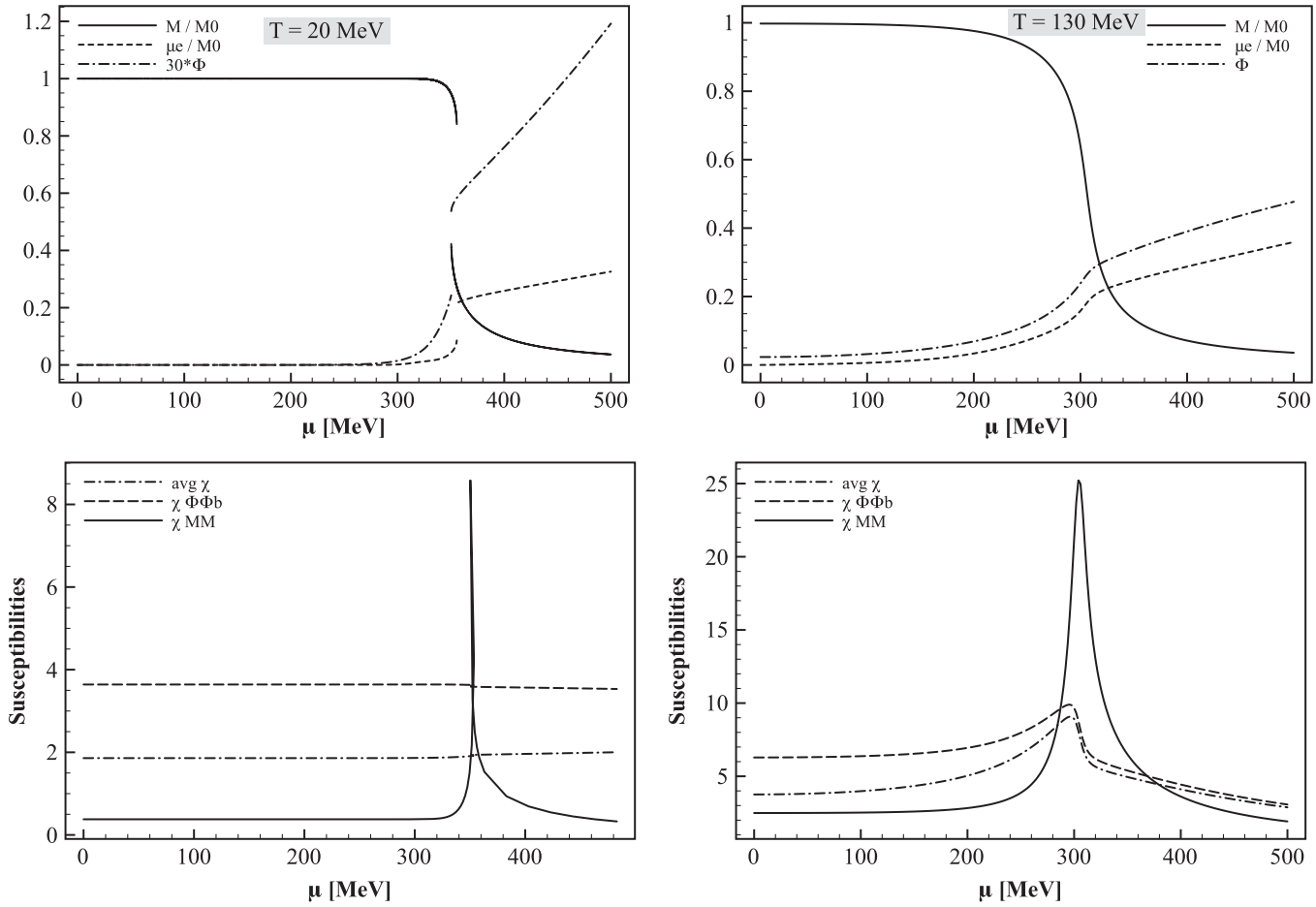

FIG. 2. Upper panel: constituent quark mass at $p = 0$, a Polyakov loop and electron chemical potential as a function of the quark chemical potential μ, computed at $T = 20$ MeV (left panel) and $T = 130$ MeV (right panel). M_0 denotes the constituent quark mass at $p = 0$ and $T = 0$, $M_0 = 335$ MeV. In both cases $N = 0$ and it is not shown. Lower panel: susceptibilities at $T = 20$ MeV (left panel) and $T = 130$ MeV (right panel) as a function of the quark chemical potential. Solid line: χ_{MM}. Dashed line: $\chi_{\Phi\bar{\Phi}}$. Dot-dashed line: $\bar{\chi}$.

show the same quantities at $T = 130$ MeV in the right panel.

Our results can be interpreted by assuming that at low temperatures the $Z(3)$ symmetry is not spontaneously broken, both at low and at high chemical potentials. The nonzero value of Φ can be related to the existence of dynamical quarks in the system that break explicitly the center symmetry. The fact that $\Phi \ll 1$ means that in the ground state colored quarks are suppressed [they have a finite $Z(3)$ charge], and the main contribution to the free energy is due to the $Z(3)$-invariant multiquark states that are states with a zero $Z(3)$ charge. This point can be clarified by studying the thermal population of the quasiquark excitations at low temperature. To this end we compute the quark number density n_q,

$$n_q = -\frac{\partial \Omega}{\partial \mu}, \tag{38}$$

as a function of the chemical potential at fixed temperature. The result is shown in Fig. 3. Evaluation of the derivative of Ω defined in Eq. (24) leads to the expression

$$n_q = \frac{3}{\pi^2}\int_0^\infty p^2 dp\left[\frac{g_{+-}}{f_{+-}} + \frac{g_{--}}{f_{--}} - \frac{g_{++}}{f_{++}} - \frac{g_{-+}}{f_{-+}}\right], \tag{39}$$

where we have introduced the functions

$$f_{\pm\pm} = 1 + 3\Phi e^{-\beta(E_\pm \pm \mu)} + 3\Phi e^{-2\beta(E_\pm \pm \mu)} + e^{-3\beta(E_\pm \pm \mu)}, \tag{40}$$

$$g_{\pm\pm} = \Phi e^{-\beta(E_\pm \pm \mu)} + 2\Phi e^{-2\beta(E_\pm \pm \mu)} + e^{-3\beta(E_\pm \pm \mu)}, \tag{41}$$

and $E_\pm$ are defined in Eq. (25). The addenda in the right-hand side of Eq. (39) correspond, respectively, to up quarks, down quarks, up antiquarks, and down antiquarks. If we put by hand $\Phi = 1$ in Eq. (39) we recover the usual expression of the NJL model,

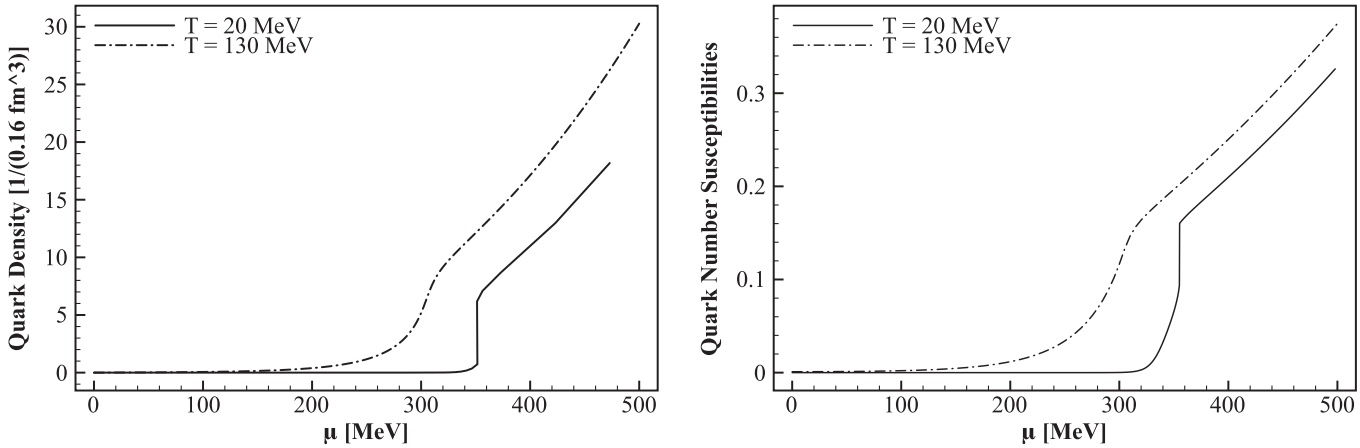

FIG. 3. Left panel: quark number densities, in units of the nuclear saturation density $\rho_0 = 0.16\ \mathrm{fm}^{-3}$, as a function of the quark chemical potential μ at $T = 20$ MeV (dashed line) and $T = 130$ MeV (dot-dashed line). Right panel: dimensionless quark number susceptibilities as a function of the quark chemical potential μ at $T = 20$ MeV (dashed line) and $T = 130$ MeV (dot-dashed line).

$$n_{q,\mathrm{NJL}} = \frac{3}{\pi^2}\int_0^\infty p^2 dp\Big[\frac{1}{1+e^{\beta(E_+-\mu)}}+\frac{1}{1+e^{\beta(E_--\mu)}} - \frac{1}{1+e^{\beta(E_++\mu)}}-\frac{1}{1+e^{\beta(E_-+\mu)}}\Big], \tag{42}$$

where the 3 overall counts the number of colors. Equation (42) is the number density of a free fermion gas; it shows that in the zero temperature limit and $\mu > M$, M denoting the constituent quark mass, the ground state of the NJL model is made of Fermi spheres of red, green, and blue quarks. Moreover at small but nonvanishing temperatures the thermal excitations over the Fermi spheres are still quarks.

Now we compare Eq. (42) with the analogous result of the PNJL model. At low temperature we have $\Phi \ll 1$; therefore, for a rough analysis we can put $\Phi = 0$ in Eq. (39). We are left with the expression:

$$n_{q,\mathrm{PNJL}} = \frac{3}{\pi^2}\int_0^\infty p^2 dp\Big[\frac{1}{1+e^{3\beta(E_+-\mu)}}+\frac{1}{1+e^{3\beta(E_--\mu)}} - \frac{1}{1+e^{3\beta(E_++\mu)}}-\frac{1}{1+e^{3\beta(E_-+\mu)}}\Big]. \tag{43}$$

The above equation is valid for every value of μ. In the limit $T \to 0$ and for $\mu > M$, with M the constituent quark mass, it gives the equation obtained in the NJL model that is a ground state of Fermi spheres of red, green, and blue quarks at the chemical potential μ. If we introduce a small temperature, then the thermal excitations are not quarks but the $Z(3)$ symmetric three-quark states, that is states made of one red quark, one green quark, and one blue quark. This is clear from the above Eq. (43) by looking at the arguments of the exponentials in the four addenda. Each of the addenda corresponds to the occupation number of fermions with energy given by $3E_\pm - 3\mu$ which is exactly the energy of the lightest $Z(3)$ symmetric state, namely [see Eqs. (28)–(30)],

$$E_{\mathrm{red}} + E_{\mathrm{green}} + E_{\mathrm{blue}} = 3E_\pm - 3\mu, \tag{44}$$

the sign depending on the flavor we consider (E_+ corresponds to up quarks, E_- to down quarks). The same result holds for antiquarks, simply by replacing $\mu \to -\mu$. The combination (44) is exactly the argument of the exponentials in Eq. (43).

To summarize: For the parametrization I the ground state of PNJL quark matter in the regime of low temperature $T \ll M$ and $\mu > M$ is made of Fermi spheres of quarks, and the thermal excitations above the aforementioned Fermi spheres are the three-quark states, neutral with respect to $Z(3)$.

For completeness, in the right panel of Fig. 3 we plot the dimensionless quark number susceptibilities, χ_q, defined as

$$\chi_q = -\frac{1}{\Lambda^2}\frac{\partial^2\Omega}{\partial\mu^2}, \tag{45}$$

where Λ is the form factor momentum scale in Eq. (14), and Ω is the PNJL free energy given by Eq. (24).

B. Case I: Phase diagram in the $\mu - T$ plane

In Fig. 4 we summarize the phase diagram of the model in the $\mu - T$ plane with the parametrization I. The thin line corresponds to the chiral crossover; the thick line is the first order chiral transition. We identify the peaks (or the local maxima) in the susceptibilities with the phase transitions. In particular, the chiral crossover is related to the peak of χ_{MM} in Eq. (36); on the other hand following Ref. [30] we identify the peak of the average susceptibility $\bar{\chi}$ defined in Eq. (37) with the Polyakov loop crossover.

From the qualitative point of view the phase diagram does not differ from our previous result [41] obtained in the sharp cutoff regularization scheme. The chiral crossover at $\mu = 0$ is located at $T_c = 215$ MeV, to be compared with

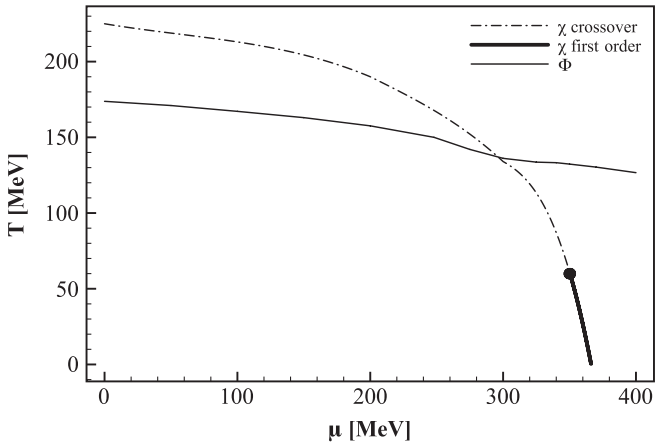

FIG. 4. Phase diagram of the neutral two flavor PNJL model. The dot-dashed line corresponds to the chiral crossover; the bold solid line is the first order transition. The thin solid line denotes the deconfinement crossover.

our previous work [41] $T_c = 206$ MeV. The critical end point is only slightly shifted: in this work we find

$$(\mu_E, T_E) \approx (350, 55) \text{ MeV}. \tag{46}$$

This result has to be compared with [41]

$$(\mu_E, T_E) \approx (340, 80) \text{ MeV}, \qquad \text{sharp cutoff}. \tag{47}$$

Finally at $T = 0$ we find that the chiral crossover occurs at $\mu = 370$ MeV, while in our previous work we have found $\mu = 350$ MeV.

We now discuss the Polyakov loop crossover line, corresponding to the thin solid line in Fig. 4. At small values of the quark chemical potential the peaks of the averaged susceptibility are well pronounced, see, for example, Fig. 1. As μ is increased, the peaks of $\bar{\chi}$ as well as of the diagonal $\chi_{\Phi\Phi}$, $\chi_{\bar{\Phi}\bar{\Phi}}$ and off-diagonal $\chi_{\bar{\Phi}\Phi}$ susceptibilities are broadened and the crossover is dilute over a wide interval of temperatures; see the right panel of Fig. 1. In the window of chemical potential studied in this paper, $0 \leq \mu \leq 500$ MeV, we are still able to observe maxima of $\bar{\chi}$ (as well as for the other susceptibilities) as a function of the temperature at a fixed value of μ; the width of the maxima increases as μ is increased. Therefore we expect that at high values of μ and T the peaks of $\bar{\chi}$ will be very dilute, meaning that the crossover disappears in the model under consideration. This result changes if we consider μ dependent coefficients of the Polyakov loop effective potential as we discuss later.

We finally notice that our results for the $Z(3)$ crossover are in qualitative agreement with the results obtained in Ref. [30], where the authors study the phase diagram and the susceptibilities of the PNJL model with quarks at the same chemical potential, and with a polynomial form of the Polyakov loop effective potential $\mathcal{U}$. This suggests that the $Z(3)$ crossover is not mainly governed by the specific form of $\mathcal{U}$ or by electrical neutrality, but by the assumption that the deconfinement scale $\bar{T}_0$ in $\mathcal{U}$ is kept independent on μ in this calculation.

C. Case II: Critical points

From the qualitative point of view, the case with $\bar{T}_0 = 270$ MeV does not differ from the previously analyzed case II. Therefore we simply give the coordinates of the critical points obtained in this case. At $\mu = 0$ we find the chiral crossover at $T = 219$ MeV and the $Z(3)$ crossover at $T = 211$ MeV. The critical end point coordinates are

$$(\mu_E, T_E) \approx (336, 103) \text{ MeV}, \qquad \bar{T}_0 = 270 \text{ MeV}. \tag{48}$$

D. Case III: Critical points and phase structure

We now discuss the results obtained in case III in which we assume both a μ and a N_f dependence of the parameter $\bar{T}_0$ of the Polyakov loop potential, see Eq. (8). Our main goal is to emphasize the differences between case III and case I. The main difference arises at low temperature and high chemical potential, so we focus on this regime. In Fig. 5 we plot on the left panel the constituent quark mass at $p = 0$ and the expectation value of Φ as a function of μ at $T = 20$ MeV, with the related susceptibilities, for case III, and compare these results with those obtained in case I at the same temperature (right panel). We have verified that qualitatively the picture does not change if we lower the temperature to the order of 1 MeV.

At $\mu = 0$ the critical temperatures are equal to those computed in case I [simply because $\bar{T}_0(\mu = 0) = 208$ MeV]. Moreover the coordinates of the critical end point are

$$(\mu_E, T_E) = (339, 53) \text{ MeV}, \qquad \bar{T}_0 = \bar{T}_0(\mu). \tag{49}$$

The data on Φ corresponding to the parametrization III show that the case $\bar{T}_0 = \bar{T}_0(\mu)$ is quite different from the case $\bar{T}_0 = 208$ MeV. In case III (left panel) in correspondence with the chiral transition at $\mu \equiv \mu_c \approx 350$ MeV the Polyakov loop has a net jump from $\Phi \ll 1$ at $\mu = \mu_c - 0^+$ to a definitely nonzero value $\Phi \approx 0.3$ at $\mu = \mu_c + 0^+$. Since the contribution of the one- and two-quark states [$Z(3)$ charges] to the free energy is multiplied by 3Φ, see Eq. (24), and in the present case 3Φ is of the order of unity, the weight of the $Z(3)$ charges in the free energy is the same of the weight of the three-quark states. This behavior is different from what we have found in the case of $\bar{T}_0 = 208$ MeV. The similarity between the two cases is partially recovered if we consider temperatures of the order of 1 MeV; in this case we find a narrow window in μ where 3Φ is of the order of 0.1, revealing a ground state in which the leading contribution to the free energy comes from the thermal excitations of $Z(3)$ neutral states. We discuss this point in more detail in the following section. Finally the analysis of the peaks of the susceptibilities $\chi_{\bar{\Phi}\Phi}$ and $\bar{\chi}$ (lower left panel of Fig. 5) reveals that the $Z(3)$ crossover occurs at $\mu \approx 460$ MeV.

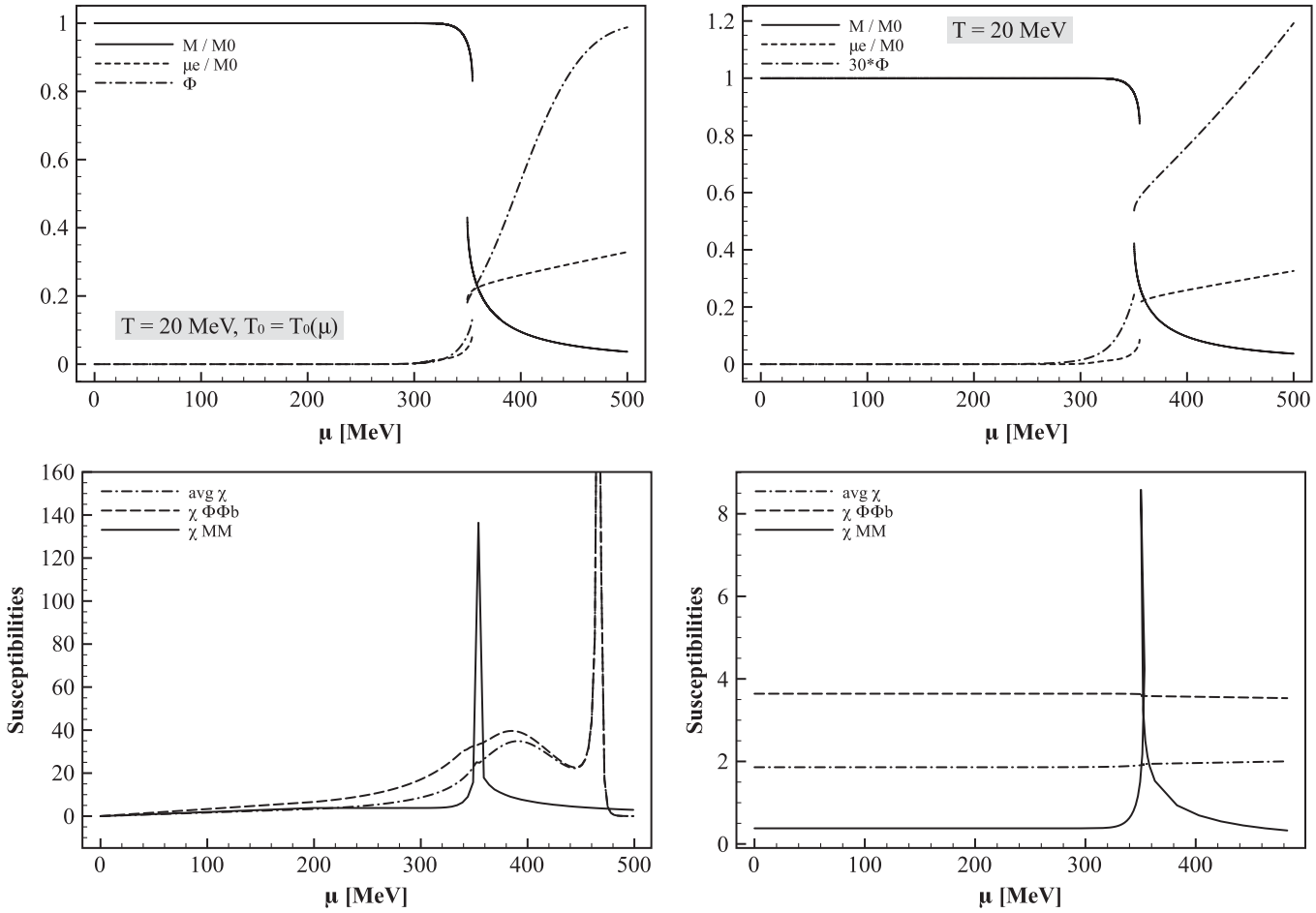

FIG. 5. Upper panel: constituent quark mass at $p = 0$, a Polyakov loop and electron chemical potential as a function of the quark chemical potential μ, computed at $T = 20$ MeV in case III (left panel) and case I (right panel, shown for comparison with case III; it is the same plot shown in Fig. 2). M_0 denotes the constituent quark mass at $p = 0$, $\mu = 0$ and $T = 0$, $M_0 = 335$ MeV. In both cases $N = 0$ and it is not shown. Lower panel: susceptibilities at $T = 20$ MeV in case III (left panel) and case II (right panel). Solid line: χ_{MM}. Dashed line: $\chi_{\Phi\bar{\Phi}}$. Dot-dashed line: $\bar{\chi}$.

V. COMPARISON BETWEEN THE TWO SCENARIOS

In this section we compare the qualitative picture that arises from the study of the phase diagram of the neutral PNJL model within two scenarios: the first one corresponds to keeping an independent $\bar{T}_0$, case I; the second one corresponds to keeping a μ-dependent $\bar{T}_0$, case III.

The results that we have discussed in the previous sections show that the phase diagram of the PNJL model in case I at low temperatures is similar to the phase diagram obtained in the large N_c approximation of QCD, see Refs. [45,46]. At low temperatures the latter phase diagram consists of two regions: the first one at low values of μ, defined as the *confined phase* and characterized by $\Phi = 0$ and a vanishing baryon density, and the second one at large values of μ called *quarkonia* in which $\Phi = 0$ but the baryon density is not vanishing. Finally at high temperature one finds the *deconfined phase* with $\Phi \neq 0$ and a nonvanishing baryon density. In the quarkyonic phase the free energy is that of free quarks, but the thermal excitations are those of baryons. Our previous discussion and Figs. 2 and 3 show that this happens even in the PNJL model in the low temperature regime. Therefore the PNJL model with parametrization I approximately reproduces the large N_c phase diagram at low temperatures, if one interprets the state with $\Phi \ll 1$ at high μ with the quarkyonic phase of large N_c. This fact has already been noticed in a study of the three flavor model by Fukushima [33] where the author has suggested to identify the low temperature–high density ground state of the model as the quarkyonic phase of large N_c QCD. Our results strengthen this idea and thus suggest that the quarkyoniclike ground state of the low temperature–high density PNJL model is not a peculiarity of the three flavor case, but it seems to be a characteristic of the PNJL model itself, as far as we do not include an explicit μ dependence into the coefficients of $\mathcal{U}$ (we discuss this case in a next section). The main difference between large N_c and PNJL is that in the latter model one can excite one- and

two-quark states [that is $Z(3)$ charges] if the temperature is high enough. As a consequence, the deconfinement transition observed in the large N_c model at high temperature and high chemical potential is replaced in the present model by a smooth $Z(3)$ crossover.

In Fig. 6 we show a cartoon phase diagram of the neutral two flavor PNJL model and a comparison with that obtained in the large N_c approximation [45]. The bold line denotes the chiral crossover as well as the chiral first order transition. The thin line corresponds to the deconfinement crossover. Both of these lines are the same as those we have shown in Fig. 4. Since this is simply a cartoon we do not distinguish between the crossover (small μ) and first order transition (higher values of μ). In the PNJL model the quark density does not vanish at any finite temperature, even if the small chemical potential n_q is very small at low temperature (see Fig. 3). To compare the phase diagram of the PNJL model with that of the large N_c approximation we need a criterion to say if n_q is zero or not. Analogously to Ref. [33] we identify the n_q crossover with the value of μ corresponding to the inflection point of the quark density. We find that the n_q crossover defined in this way coincides with the chiral crossover as in Ref. [33]. Therefore the chiral crossover line in Fig. 6 represents the density crossover as well. In the chiral broken phase and at low temperature $n_q \approx 0$. On the other hand $n_q \neq 0$ in correspondence to the chiral symmetric phase at low temperature. At high temperature $n_q \neq 0$ both in the chiral broken and in the chiral restored phases.

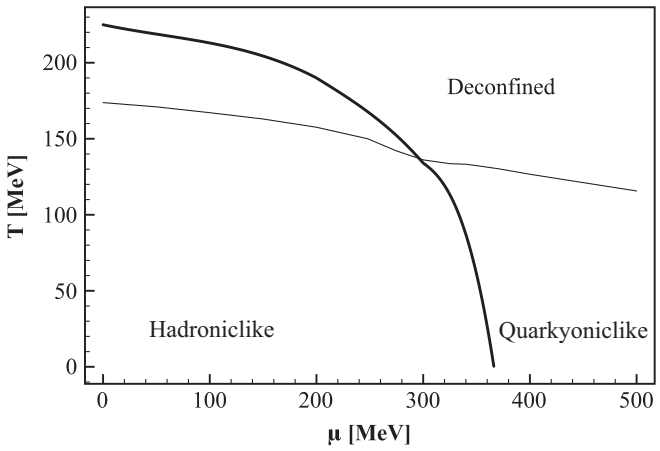

FIG. 6. Cartoon phase diagram of the neutral two flavor PNJL model and comparison with that obtained in the large N_c approximation [45]. The bold line denotes the chiral crossover as well as the chiral first order transition. The thin line corresponds to the deconfinement crossover. Both of these lines are the same as those we have shown in Fig. 4. The n_q crossover coincides with the chiral one. At low temperature we have $\Phi \approx 0$ and $n_q \approx 0$ in the chiral broken phase, in agreement with the hadronic phase of Ref. [45]. At low temperature and in the chiral symmetric phase we find $\Phi \approx 0$ and $n_q \neq 0$ in agreement with the quarkyonic phase [45]. For these reasons we have called the two low temperature regions *hadroniclike* and *quarkyoniclike*, respectively.

At low temperature we have $\Phi \approx 0$ both on the left and on the right of the dashed line; see Figs. 1 and 2. At low temperature the region with broken chiral symmetry has the same characteristics of the hadron phase found in Ref. [45]; on the other hand at low temperature the region on the right of the dashed line has the same characteristics of the quarkyonic phase found in Ref. [45]. For these reasons we have called the two regions *hadroniclike* and *quarkyoniclike*, respectively. We stress that this analogy holds strictly speaking only at low temperature (for temperatures of the order of 100 MeV $n_q \neq 0$ even in the chiral broken phase, see Fig. 3). Finally at high temperature [above the $Z(3)$ transition line] we have both Φ of order of unity and $n_q \neq 0$. In analogy to the terminology of Ref. [45] we call this region of the phase diagram the *deconfinedlike* phase.

We briefly compare the results discussed above in relation to case I with those obtained in the large N_c approximation and at $T = 0$ in Ref. [48], where the author discusses a gap in the spectrum of quarkyonic matter within a model. Such a gap is given by the pion mass, M_π, which becomes larger as μ is increased. Even if the values of M_π as a function of μ computed in Ref. [48] might differ from the nonlocal PNJL ones, the calculations of M_π carried out in Refs. [40,41] using the local NJL model show that the qualitative behavior of M_π as a function of μ is the same in the two models. Thus in the PNJL model we expect a large pion mass at large μ as well. However this mass does not correspond to the gap in the excitations spectrum in our model. As a matter of fact in the quarkyoniclike region of the phase diagram in Fig. 6 the three-quark states can be excited; each quark has a constituent mass $M(p)$ given by Eq. (21) and plotted in Figs. 1 and 2; hence the three-quark state has a mass $3M(p)$ which at small quark momenta and large μ is of the order of 10 MeV. Therefore in our case a gap in the spectrum still exists but it is given by the three-quark state mass which is much lighter than M_π.

We now turn on the parametrization III. As discussed in the previous section, the small chemical potential region of the phase diagram in case III is qualitatively similar to that obtained in case I, therefore we focus on the low temperature/large chemical potential region from now on. In Fig. 7 we draw the low temperature phase diagram of the PNJL model with parametrization III. The bold line denotes the chiral transition; the thin line corresponds to the $Z(3)$ transition. As in the previous section the transition lines are computed by looking at the peaks of the chiral and $\bar{\chi}$ susceptibilities. The diagram in Fig. 7 should be compared with the analogous diagram obtained for the parametrization I which is shown in Fig. 4. The main effect of choosing the parameter $\bar{T}_0$ as a μ dependent one in the Polyakov loop potential is the lowering of the $Z(3)$ tran-

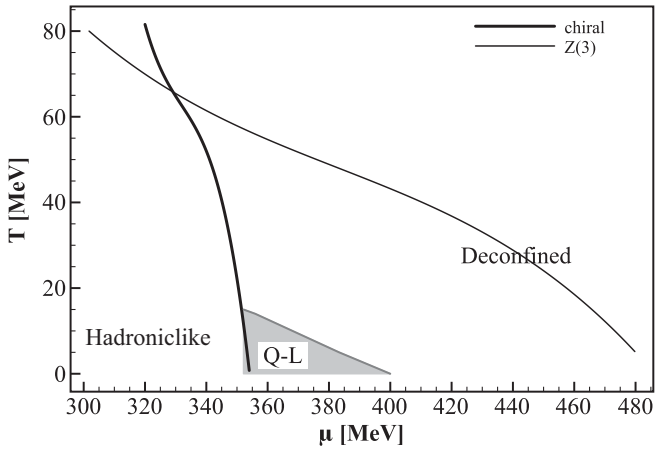

FIG. 7. Low temperature phase diagram of the PNJL model with parametrization III. The bold line denotes the chiral transition. The thin line corresponds to the $Z(3)$ transition. The shaded region denoted by Q-L corresponds to the zone of the quarkyoniclike state of matter.

sition line. Moreover the wide quarkyoniclike window in Fig. 6 is shrunk to a small region in Fig. 7. At low temperature it is enough to reach a chemical potential of the order of 500 MeV to have $\Phi \approx 1$ and a net quark density; both of these characteristics define the deconfined phase of Fig. 6 [45]. Even if we have used the particular form $\bar{T}_0(\mu)$ suggested in Ref. [28] we are confident that the aforementioned results are simply due to the lowering of the deconfinement scale $\bar{T}_0$ as μ is increased and not to the detailed analytical form of $\bar{T}_0(\mu)$. Thus our picture should be qualitatively robust.

Before closing this section we make a brief comment on the possible study of the scenarios discussed above on lattice. Recently the density of states (DOS) method has been used to investigate the QCD phase transition at large μ [13]. In this paper the QCD phase diagram is mapped by studying the plaquette expectation value in the $\mu - T$ plane. Although the lattice size implemented in [13] is relatively small and a finite volume study is still missing, so that the results should be taken as preliminary, an interesting phase transition is observed as μ crosses a critical value μ_c at a fixed temperature. Moreover the quark number shows a sudden rise as μ reaches μ_c. The qualitative behavior is similar to the PNJL model, see Figs. 1–3. In the PNJL calculation with parametrization of cases I and II (fixed values of T_0) at low temperature and in the correspondence of the chiral crossover a small jump of the Polyakov loop occurs, the true $Z(3)$ crossover being shifted to larger values of μ. On the other hand, in case III with a μ-dependent T_0, a net rise of Φ occurs in correspondence of the chiral crossover. It would be very interesting if by means of the DOS method one could compute the expectation value of the Polyakov loop, as well as the chiral and the Polyakov loop susceptibilities, in the low temperature regime as a function of μ. This lattice calculation might improve the understanding of the new low temperature/large chemical potential state of matter claimed in [13], and at the same time it would allow one to distinguish between the two PNJL scenarios discussed in this paper.

VI. CONCLUSIONS

In this paper we have investigated the landscape of the possible phases of the neutral two flavor PNJL model. We have considered the logarithmic effective potential of the Polyakov loop $\mathcal{U}$ [23,25], see Eq. (3), and a nonlocal interaction in the quark sector, see Eqs. (12)–(14). Our main results are summarized in Figs. 4 and 7. Figure 4 corresponds to a fixed value of $\bar{T}_0$ in the Polyakov loop effective potential. In this case the phase diagram is qualitatively similar to that obtained in the large N_c approximation of QCD [45].

In particular, at high chemical potential and low temperature we find a phase in which the main contribution to the thermal quark population is given by $Z(3)$ neutral states, that is three-quark states made of one red quark, one green quark, and one blue quark. This characteristic resembles the quarkyonic phase of Ref. [45]. The quarkyoniclike structure of the ground state of the PNJL model has already been noticed in Ref. [33] in non-neutral and three flavor version of the model. Moreover the $Z(3)$ transition line has already been studied in Ref. [30] with a different effective potential for the Polyakov loop and in a non-neutral state. The results of Ref. [30] are qualitatively similar to ours. Therefore we suggest that the quarkyoniclike state of matter is a feature of the PNJL model, independent to the number of flavors and to the difference of the chemical potentials between quarks, as far as a μ dependence of the coefficients of $\mathcal{U}$ is not considered.

In Fig. 7 we show the phase diagram of the model when a μ dependence of the coefficients of the effective potential of the Polyakov loop is introduced. We have used the analytic form suggested in Ref. [28]. The main results are the lowering of the $Z(3)$ transition line of Fig. 4, and the shrinking of the quarkyoniclike phase window of Fig. 4. We have used the form of $\bar{T}_0(\mu)$ of Ref. [28]. We believe that the result is rather robust as it does not follow from such a detailed form but only from the lower scale of deconfinement when μ increases.

We have not considered in this work for simplicity the possibility of color superconductivity at high μ [59,60]. At first sight it could seem that the results found with parametrizations I and II, i.e., a quarkyoniclike phase at high chemical potential and low temperature, exclude the possibility of a superconductive gap in the spectrum. This reasoning could be supported by the observation that the quarkyoniclike phase is similar to a confined phase, differing from the latter only for a nonzero value of the quark density. Such a conclusion is not necessarily true. As a matter of fact, even if not noticed explicitly in Ref. [25] for

the two flavor and in [37,42] for the three flavor models where the color superconductivity has been kept into account, in the quarkyoniclike region (high μ and small T) the minimization of the thermodynamic potential leads to a phase where quarks have a color superconductive gap in the spectrum. It is the 2SC gap [59] in the two flavor case, and the CFL gap [60] in the three flavor case. Therefore the realization of a color superconductive phase in the PNJL models at high μ and small T is not forbidden in principle, even if the ground state has a quarkyonic structure.

An interesting investigation is the computation of the spectra of the mesonic and baryonic thermal excitations in the quarkyoniclike phase of the PNJL model, and we compare them with those obtained in a different model [48] that mimics QCD in the large N_c approximation. We are now working on this topic and the results will be the object of a forthcoming paper.

ACKNOWLEDGMENTS

We acknowledge K. Fukushima, M. Hamada, M. Huang, O. Kiriyama, T. Kunihiro, V. A. Miransky, C. Sasaki, A. Schmitt, I. Shovkovy, and W. Weise for discussions made during the Workshop "New Frontiers in QCD 2008." Moreover, we have benefited from a discussion with K. Redlich during the aforementioned Workshop which has stimulated the main part of the present work. We finally thank P. Cea and L. Cosmai for enlightening discussions and D. Blaschke for useful correspondence.

[1] Y. Aoki, Z. Fodor, S. D. Katz, and K. K. Szabo, Phys. Lett. B **643**, 46 (2006).
[2] C. Schmidt, Proc. Sci., LAT2006 (2006) 021 [arXiv:hep-lat/0610116].
[3] O. Philipsen, Proc. Sci., LAT2005 (2006) 016 [arXiv:hep-lat/0510077]; JHW2005 (2006) 012.
[4] U. M. Heller, Proc. Sci., LAT2006 (2006) 011 [arXiv:hep-lat/0610114].
[5] S. Ejiri, Phys. Rev. D **69**, 094506 (2004).
[6] K. Splittorff, Proc. Sci., LAT2006 (2006) 023.
[7] K. Splittorff and J. J. M. Verbaarschot, Phys. Rev. Lett. **98**, 031601 (2007).
[8] C. R. Allton, S. Ejiri, S. J. Hands, O. Kaczmarek, F. Karsch, E. Laermann, and C. Schmidt, Phys. Rev. D **68**, 014507 (2003).
[9] C. R. Allton *et al.*, Phys. Rev. D **66**, 074507 (2002).
[10] C. R. Allton *et al.*, Phys. Rev. D **71**, 054508 (2005).
[11] Z. Fodor, S. D. Katz, and K. K. Szabo, Phys. Lett. B **568**, 73 (2003).
[12] Z. Fodor and S. D. Katz, J. High Energy Phys. 03 (2002) 014.
[13] Z. Fodor, S. D. Katz, and C. Schmidt, J. High Energy Phys. 03 (2007) 121.
[14] E. Laermann and O. Philipsen, Annu. Rev. Nucl. Part. Sci. **53**, 163 (2003).
[15] P. de Forcrand and O. Philipsen, Nucl. Phys. **B673**, 170 (2003).
[16] M. D'Elia, F. Di Renzo, and M. P. Lombardo, Phys. Rev. D **76**, 114509 (2007).
[17] M. D'Elia and M. P. Lombardo, Phys. Rev. D **70**, 074509 (2004).
[18] M. D'Elia and M. P. Lombardo, Phys. Rev. D **67**, 014505 (2003).
[19] Y. Nambu and G. Jona-Lasinio, Phys. Rev. **122**, 345 (1961); **124**, 246 (1961).
[20] U. Vogl and W. Weise, Prog. Part. Nucl. Phys. **27**, 195 (1991); S. P. Klevansky, Rev. Mod. Phys. **64**, 649 (1992); T. Hatsuda and T. Kunihiro, Phys. Rep. **247**, 221 (1994); M. Buballa, Phys. Rep. **407**, 205 (2005).
[21] A. M. Polyakov, Phys. Lett. **72B**, 477 (1978); L. Susskind, Phys. Rev. D **20**, 2610 (1979); B. Svetitsky and L. G. Yaffe, Nucl. Phys. **B210**, 423 (1982); B. Svetitsky, Phys. Rep. **132**, 1 (1986).
[22] P. N. Meisinger and M. C. Ogilvie, Phys. Lett. B **379**, 163 (1996).
[23] K. Fukushima, Phys. Lett. B **591**, 277 (2004).
[24] C. Ratti, M. A. Thaler, and W. Weise, Phys. Rev. D **73**, 014019 (2006).
[25] S. Roessner, C. Ratti, and W. Weise, Phys. Rev. D **75**, 034007 (2007).
[26] S. K. Ghosh, T. K. Mukherjee, M. G. Mustafa, and R. Ray, Phys. Rev. D **77**, 094024 (2008); **73**, 114007 (2006).
[27] K. Kashiwa, H. Kouno, M. Matsuzaki, and M. Yahiro, Phys. Lett. B **662**, 26 (2008).
[28] B. J. Schaefer, J. M. Pawlowski, and J. Wambach, Phys. Rev. D **76**, 074023 (2007).
[29] C. Ratti, S. Roessner, and W. Weise, Phys. Lett. B **649**, 57 (2007).
[30] C. Sasaki, B. Friman, and K. Redlich, Phys. Rev. D **75**, 074013 (2007); **75**, 054026 (2007).
[31] E. Megias, E. Ruiz Arriola, and L. L. Salcedo, Phys. Rev. D **74**, 114014 (2006); **74**, 065005 (2006).
[32] Z. Zhang and Y. X. Liu, Phys. Rev. C **75**, 064910 (2007).
[33] K. Fukushima, Phys. Rev. D **77**, 114028 (2008).
[34] Y. Sakai, K. Kashiwa, H. Kouno, and M. Yahiro, Phys. Rev. D **77**, 051901 (2008).
[35] Y. Sakai, K. Kashiwa, H. Kouno, and M. Yahiro, Phys. Rev. D **78**, 036001 (2008).
[36] K. Kashiwa, Y. Sakai, H. Kouno, M. Matsuzaki, and M. Yahiro, arXiv:0804.3557.
[37] M. Ciminale, G. Nardulli, M. Ruggieri, and R. Gatto, Phys. Lett. B **657**, 64 (2007).
[38] W. j. Fu, Z. Zhang, and Y. x. Liu, Phys. Rev. D **77**, 014006 (2008).
[39] M. Ciminale, R. Gatto, N. D. Ippolito, G. Nardulli, and M. Ruggieri, Phys. Rev. D **77**, 054023 (2008).

[40] H. Hansen, W. M. Alberico, A. Beraudo, A. Molinari, M. Nardi, and C. Ratti, Phys. Rev. D **75**, 065004 (2007).
[41] H. Abuki, M. Ciminale, R. Gatto, N. D. Ippolito, G. Nardulli, and M. Ruggieri, Phys. Rev. D **78**, 014002 (2008).
[42] H. Abuki, M. Ciminale, R. Gatto, G. Nardulli, and M. Ruggieri, Phys. Rev. D **77**, 074018 (2008).
[43] G. A. Contrera, D. Gomez Dumm, and N. N. Scoccola, Phys. Lett. B **661**, 113 (2008).
[44] D. Blaschke, M. Buballa, A. E. Radzhabov, and M. K. Volkov, arXiv:0705.0384.
[45] L. McLerran and R. D. Pisarski, Nucl. Phys. **A796**, 83 (2007).
[46] Y. Hidaka, L. D. McLerran, and R. D. Pisarski, Nucl. Phys. **A808**, 117 (2008).
[47] L. Y. Glozman and R. F. Wagenbrunn, Phys. Rev. D **77**, 054027 (2008).
[48] L. Y. Glozman, arXiv:0803.1636.
[49] S. M. Schmidt, D. Blaschke, and Yu. L. Kalinovsky, Phys. Rev. C **50**, 435 (1994).
[50] R. D. Bowler and M. C. Birse, Nucl. Phys. **A582**, 655 (1995).
[51] D. Blaschke, G. Burau, Yu. L. Kalinovsky, P. Maris, and P. C. Tandy, Int. J. Mod. Phys. A **16**, 2267 (2001).
[52] D. Gomez Dumm, D. B. Blaschke, A. G. Grunfeld, and N. N. Scoccola, Phys. Rev. D **73**, 114019 (2006).
[53] D. N. Aguilera, D. Blaschke, H. Grigorian, and N. N. Scoccola, Phys. Rev. D **74**, 114005 (2006).
[54] H. Grigorian, Phys. Part. Nucl. Lett. **4**, 223 (2007).
[55] D. Ebert and K. G. Klimenko, Eur. Phys. J. C **46**, 771 (2006).
[56] D. Ebert, K. G. Klimenko, and H. Toki, Phys. Rev. D **64**, 014038 (2001); D. Ebert, V. V. Khudyakov, V. C. Zhukovsky, and K. G. Klimenko, Phys. Rev. D **65**, 054024 (2002).
[57] D. Ebert, K. G. Klimenko, A. V. Tyukov, and V. C. Zhukovsky, arXiv:0804.0765.
[58] L. y. He, M. Jin, and P. f. Zhuang, Phys. Rev. D **71**, 116001 (2005).
[59] R. Rapp, T. Schafer, E. V. Shuryak, and M. Velkovsky, Phys. Rev. Lett. **81**, 53 (1998); M. G. Alford, K. Rajagopal, and F. Wilczek, Phys. Lett. B **422**, 247 (1998).
[60] M. G. Alford, K. Rajagopal, and F. Wilczek, Nucl. Phys. **B537**, 443 (1999).